Pergamon

PII: S0043-1354(98)00149-3

Wat. Res. Vol. 32, No. 12, pp. 3747–3755, 1998
© 1998 Elsevier Science Ltd. All rights reserved
Printed in Great Britain
0043-1354/98 $19.00 + 0.00

THE ACCURACY OF OXYGEN FLUX MEASUREMENTS USING MICROELECTRODES

KJETIL RASMUSSEN*Ⓜ and ZBIGNIEW LEWANDOWSKI†Ⓜ

Center for Biofilm Engineering, 409 Cobleigh Hall, P.O. Box 173980, Montana State University-Bozeman, Bozeman, MT 59717-3980, U.S.A.

(First received January 1997; accepted in revised form March 1998)

Abstract—An electrochemical analog of a biofilm was constructed to test the accuracy of oxygen flux measurements using microelectrodes. We used a cathodically polarized graphite felt attached to the bottom of a flat plate open channel reactor as the reactive surface consuming oxygen. The oxygen flux to the felt was calculated from the polarization current. Microelectrodes were used to measure the oxygen profiles above and within the graphite felt. From the shape of the oxygen profile we evaluated the oxygen flux to the graphite felt. This provided us with two sets of data, the true oxygen flux, calculated from polarization current, and the oxygen flux estimated from microelectrode measurements. Comparing these two fluxes, for different flow velocities, showed that the fluxes evaluated from the polarization current were different from those evaluated from the oxygen profiles. The differences were likely caused by the presence of the microelectrode in the mass boundary layer and/or by the simplifying assumptions accepted in computational procedures employed to calculate oxygen fluxes. For low flow velocities, between zero and 1.0 cm s^{-1}, the differences were velocity sensitive; the higher the flow velocity, the bigger the difference. For higher flow velocities, between 1 cm s^{-1} and 3 cm s^{-1}, the flux of oxygen estimated from the microelectrode measurements was consistently approximately 80% higher than the true oxygen flux estimated from the polarization current. © 1998 Elsevier Science Ltd. All rights reserved

Key words: microelectrodes, biofilms, concentration gradients.

INTRODUCTION

Rapid development of biofilm research in environmental engineering, microbial ecology and medicine proves that this long underestimated mode of microbial growth is finally achieving the recognition that it deserves. Biofilms are intensively studied in such disparate areas as bioremediation of toxic compounds (Cunningham and Peyton, 1995; Sturman *et al*., 1995), oral hygiene (Marsh, 1995), souring of oil formations (Chen *et al*., 1994; Chen and Reinsel, 1996), microbially influenced corrosion (Hamilton, 1995; Lee *et al*., 1995) and infection of prosthetic devices (Holmes and Evans, 1986; Gristina, 1994). The kinetics of biofilm reactions are transport limited and, therefore, the substrates metabolized in biofilms and the products of these metabolic reactions form concentration gradients. The shape of these profiles are influenced by many factors, but mainly by the reaction rate and the mass transport rate of substrates to and from the biofilm. Each point of the concentration profile reflects the equilibrium between the supply of the solute by mass transport and its conversion by microbial metabolism. Therefore, the shape of the concentration profiles are sensitive to all factors influencing both reaction rate (e.g. presence of inhibitors) and mass transport rate (e.g. hydrodynamics). To study the dynamics of biofilm processes, direct measurements of concentration profiles are indispensable. The most reliable analytical tools, thus far, to measure these profiles are microelectrodes. Use of motorized micromanipulators allow the microelectrodes to be moved with high precision across biofilms. To assure the high spatial resolution of sensor positioning, the tips of the microelectrodes are necessarily in the range of a few microns. Microelectrodes are frequently the tools of choice to study kinetics of biofilm processes at microscale.

It is often assumed that because of the small tip diameters (usually a few microns) the microelectrodes do not alter the biofilm structure during measurements. However, any change of biofilm structure caused by the electrode tip could affect the results in an unpredictable way. For example, a large blunt tip could create a dent in the biofilm, allowing bulk liquid with a high concentration of substrate to penetrate into the dent and, thereby, change the shape of the substrate concentration profile. Although concentration profiles measured several times at the same locations in a biofilm rarely differ, which suggests that this method is

*Present address: Department of Biotechnology, The Norwegian University of Science and Technology, N-7034 Trondheim, Norway.

†Author to whom all correspondence should be addressed.

non-destructive, the microelectrode measurement remains invasive and the presence of the electrode in the biofilm may affect the measurement. It is important to know the magnitude of any such effect in designing biofilm experiments and to conduct the microelectrode measurements. Glud *et al.* (1994) studied the effects the presence of oxygen microelectrodes on the accuracy of oxygen profile measurements in sediments using two microelectrodes, one introduced from above the sediment and the other from below, along the same vertical axis. They reported that the microelectrode positioned above the sediments compressed the mass boundary layer by 25–45% which resulted in steeper oxygen profiles.

Due to the lack of independent methods to verify the results of microelectrode measurements, it is difficult to evaluate their accuracy. Microelectrodes are calibrated under completely mixed conditions. This means that the solute concentration is constant throughout the system and the results can not be influenced by the presence of the electrode. On the other hand, the same microelectrodes are then used to measure steep concentration gradients where their presence may disturb the local conditions. Consequently, the local concentration of the measured solute may not be the same as it would be in the absence of the electrode. Some common computational practices in the microelectrode measurement may also introduce errors in the final estimate of the reaction kinetics. For example, it is customary to assume that water is stagnant within the mass boundary layer and, therefore, the molecular diffusivity of solute is used to evaluate the mass transport rate. Our earlier work (Lewandowski *et al.*, 1995a,b; De Beer *et al.*, 1996) indicated that water is moving within the diffusion boundary layer and within the biofilm. Consequently, we know that there is convective mixing near and within biofilms and that accepting molecular diffusivity to calculate fluxes from concentration profiles introduces an error of unknown magnitude. The lack of independent measurement of concentration profiles makes it difficult to verify the results and to estimate the accuracy of microelectrode measurements.

The goal of this work was to test the accuracy of the oxygen flux measurements using dissolved oxygen microelectrodes. Dissolved oxygen microelectrodes with tip diameters typically in the range of a few microns are often used to measure oxygen profiles in biofilms (Lewandowski *et al.*, 1989; Revsbech *et al.*, 1989; Nielsen *et al.*, 1990a; Dalsgaard and Revsbech, 1992; Lewandowski *et al.*, 1993; Ramsing *et al.*, 1993; Larsen and Harremoës, 1994; Abrahamson, 1995; Dalsgaard *et al.*, 1995; Zhang *et al.*, 1995a,b), stream sediments (Christensen *et al.*, 1989; Nielsen *et al.*, 1990b), soil aggregates (Højberg *et al.*, 1994), termite guts (Brune *et al.*, 1995) and blood vessels (Clark *et al.*, 1953). The measured profiles of oxygen concentration are frequently used to evaluate the microbial respiration rate and flux of oxygen.

To test the accuracy of oxygen flux measurements using microelectrodes we have constructed an electrochemical analog of a biofilm. A piece of graphite felt was glued to the bottom of an open channel flow reactor and polarized cathodically. The graphite felt used as the reactive surface imitated a porous biofilm. Cathodic polarization resulted in dissolved oxygen consumption by an electrochemical reaction (equation 1). The rate of oxygen consumption was easily and exactly controlled by the applied polarization potential and measured by monitoring the current in the polarization circuit. Reactive surfaces are often used to study the effects of hydrodynamics on mass transfer rates in chemical reactors. The limiting current technique is commonly applied in such experiments. Hanratty (1991) used this technique to measure the wall shear stress in a pipe. Juhasz and Deen (1993) studied the mass transfer to surfaces with small reactive areas of various patterns. Dawson and Trass (1972) applied the limiting current technique to study the mass transfer rates to rough surfaces. DeBecker *et al.* (1995) defined how a periodic fluid flow influenced the mass transfer to a line electrode. Longmire *et al.* (1990) determined the diffusion coefficients of ferrocene solutes in polymeric solvents. Gao *et al.* (1995) determined how the orientation of a microdisk electrode, with respect to the gravitational field, influenced the mass transfer rates to the disk. Finally, in our laboratory Yang and Lewandowski (1995) used a mobile microelectrode based on limiting current technique to measure local mass transfer coefficients inside biofilms.

The principle of the electrochemical analog of a biofilm stems from using a reactive surface to electrochemically consume oxygen at a known and precisely controlled rate. The reactive surface is polarized cathodically and the resulting reduction of oxygen (equation 1) generates a current in the polarizing circuit

$$O_2 + 2H_2O + 4e^- \longrightarrow 4OH^-. \quad (1)$$

The current measured is proportional to the flux of oxygen:

$$I = J \cdot F \cdot A \cdot n, \quad (2)$$

where I is the current (in C s^{-1}, A) that is measured, J is the flux of oxygen (mol s^{-1} m^{-2}), F is the Faraday's constant (C mol^{-1}), A is the surface area (m^2) of the reactive surface and n is the number of electrons transferred in the reaction; four in this case.

The conditions are such that the current (I) results only from oxygen reduction. Consequently, the flux of oxygen to the reactive surface (J) can be calculated from equation 2 if the surface area is known. The surface area in equation 2 is the length

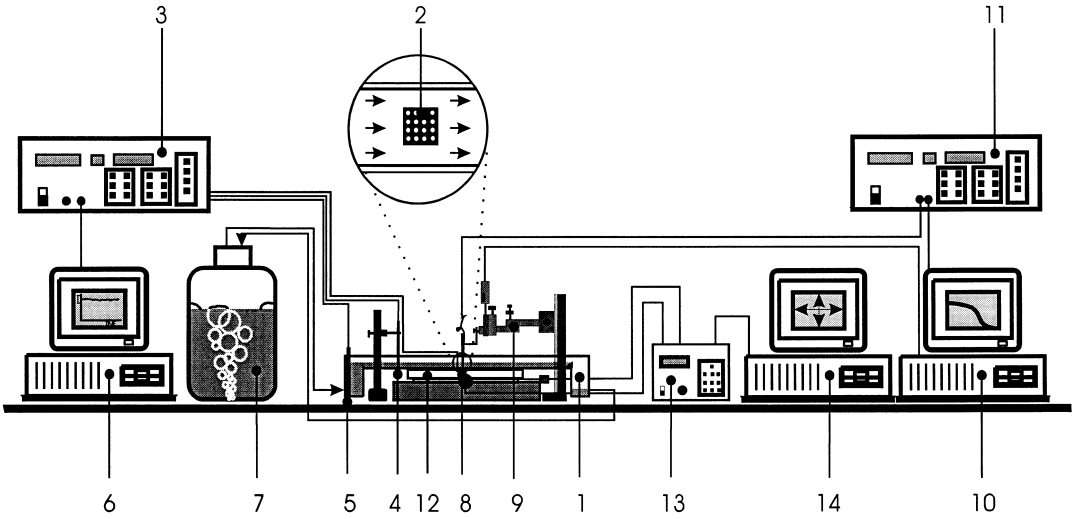


Fig. 1. Experimental setup: (1) open channel reactor, (2) graphite felt, (3) potentiostat, (4) reference electrode, (5) counter electrode, (6) computer for potentiostat operation, (7) KCl solution, (8) dissolved oxygen microelectrode, (9) micromanipulator, (10) data acquisition system, (11) picoammeter/DC voltage source, (12) X–Y micropositioner stage, (13) controller, (14) computer for stage movement.

times the width of the square shaped piece of graphite felt. The graphite felt itself has a convoluted surface area due to its porous structure. However, the surface area which appears in Fick's diffusion equations is the surface area measured perpendicularly to the flux of electroactive species and, therefore, the projection of the felt surface (length times width) was accepted in flux calculations. The flux of oxygen to the graphite felt was calculated from the measured current. Since the current was generated only by oxygen consumption, the calculated flux of oxygen was accepted as the "true" flux. Its value could then be compared with the flux measured by microelectrodes.

Fick's first law of diffusion is used to calculate the flux of oxygen from the microelectrode measurements:

$$J = D \cdot (\mathrm{d}C/\mathrm{d}X), \tag{3}$$

where D is the diffusivity of oxygen in water and $(\mathrm{d}C/\mathrm{d}X)$ is the concentration gradient; which represents the slope of the profile at the interface between the water and the biofilm, or between the water and the graphite felt in our case.

Simultaneously monitoring the current and measuring the profiles of dissolved oxygen above and within the reactive surfaces, we were able to generate two sets of data: (1) the flux of oxygen calculated from the polarization current (which is the true value) and (2) the flux of oxygen calculated from the oxygen profile. If these two fluxes are identical, our measurement system is ideal. It is expected, however, that the presence of the microelectrode in the flow field may affect the hydrodynamic and the mass boundary layers and that the simplifications in computational procedures employed to calculate the flux from oxygen profiles may introduce errors. Consequently, the oxygen flux calculated from the oxygen profiles is expected to be different than the true oxygen flux calculated from the polarizing current. The question is whether any such difference is significant.

MATERIALS AND METHODS

The experimental setup is shown in Fig. 1. The open channel reactor (1), made of polycarbonate, was 40 mm wide and 750 mm long. A 0.3 mm thick, 17×17 mm graphite felt (2) (Electrosynthesis Co. Inc., Lancaster, NY) was glued with Photo Mount (3 M, St. Paul, MN) to the bottom of the reactor 485 mm from the inlet. A potentiostat (3) (Model 273, EG&G Princeton Applied Research, Princeton, NJ) was used to polarize the graphite felt and to measure the resulting current. A standard calomel electrode (SCE) (4) (Model 13 – 620-51, Fisher Scientific, Pittsburgh, PA) was used as a reference electrode and a $1/4'' \times 12''$ graphite rod (5) (Electrosynthesis Co. Inc., Lancaster, NY) was used as a counter electrode. The potentiostat was computer controlled (6) using Model 352 Corrosion Software 1.0 (EG and G Princeton Applied Research, Princeton, NJ). The electrolyte, 0.5 M KCl solution, was recycled through the reactor by a peristaltic pump (Cole-Parmer Instrument Co., Chicago, IL) and continuously aerated in a plastic carboy (7).

The combined dissolved oxygen microelectrode and reference electrode (8) was constructed as described by

Table 1. Reynolds number for each flow velocity in the experiments

Flow velocity (cm s^{-1})	Reynolds number (Re)
0.139	30
0.408	100
0.456	100
0.694	200
1.11	300
1.99	500
2.30	600
2.78	800

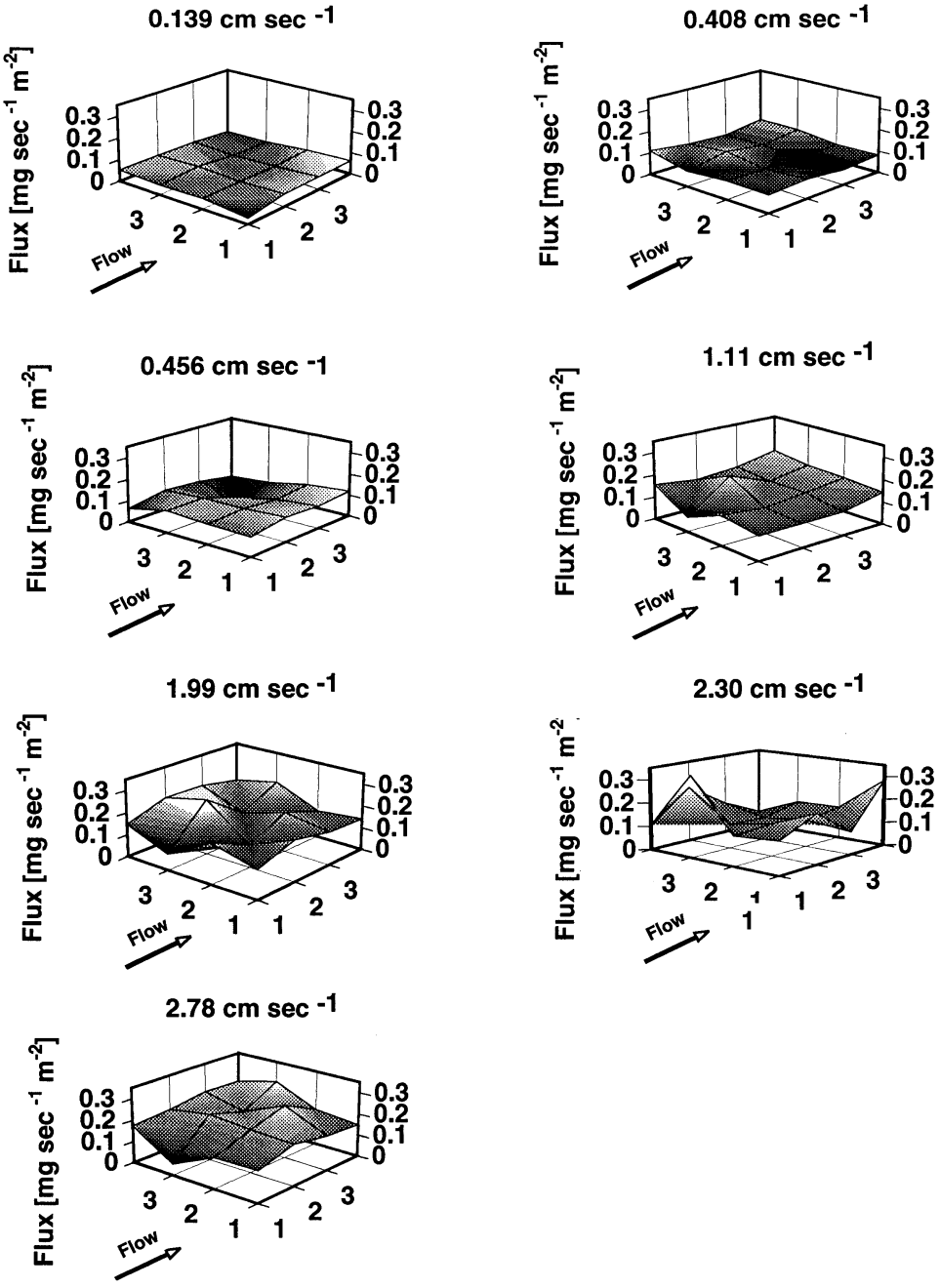


Fig. 2. Oxygen flux distribution above the graphite felt calculated from the oxygen profiles. The estimated flux is uniformly distributed at low flow velocities, but as the velocity increases the standard deviation increases as well. There is no pattern in the flux distribution.

Revsbech (1989). Each electrode was calibrated before the measurements. Electrodes failing to give a stable reading or a sufficient response time were rejected. The electrodes were mounted on a micromanipulator (9) (Model M3301L, World Precision Instruments, New Haven, CT) equipped with a stepper motor (Model 18503, Oriel, Stratford, CT) and manipulated by a controller (13) (Model 20010, Oriel, Stratford, CT) to measure oxygen concentration in 10 μm increments. The current was monitored by the computer data acquisition system (Model CIO-DAS08PGL, Computer Boards, Inc., Mansfield, MA) (10). The microelectrodes were polarized and the polarization current was measured using the Picoammeter/DC voltage source, Hewlet Packard 4140B (11). At each position of the microelectrode 22 current readings were collected at a frequency of 1 kHz. The highest and lowest readings were rejected and a standard deviation was calculated for the remaining 20 measurements. If the deviation was greater than 5% the measurement was repeated, otherwise the result was stored and the electrode was moved to the next vertical position for a new measurement. Custom-made software was used to display the oxygen profiles on the computer monitor in real time.

Dissolved oxygen profiles were collected at different locations above and within the graphite felt. The porous structure of the felt and the elasticity of the carbon fibers

Table 2. Analysis of the flux distributions in Fig. 2

Flux distributions	Flow velocity ($cm\ s^{-1}$)	Average flux ($mg\ s^{-1}\ m^{-2}$)	Standard deviation ($mg\ s^{-1}\ m^{-2}$)	Deviation as percentage of average flux (%)
(A)	0.139	0.0487	0.00911	19
(B)	0.408	0.0850	0.0137	16
(C)	0.456	0.0897	0.0207	23
(D)	1.11	0.138	0.0336	24
(E)	1.99	0.161	0.0456	28
(F)	2.30	0.152	0.0760	50
(G)	2.78	0.180	0.0483	27

made it penetrable by dissolved oxygen microelectrodes. We used an *X–Y* micropositioner stage (12) (Model CTC-462-2S, MicroKinetics, Laguna Hills, CA) to manipulate the position of the sample. The reactor was positioned on the stage and after an oxygen profile was measured at one location the electrode was raised and the stage moved the reactor to the next position for the next profile measurement. The stage was computer-controlled through a controller (13) (Model CTC-283-3, MicroKinetics, Laguna Hills, CA) with a positioning precision of 0.1 μm. The computer (14) equipped with custom-made software was used to manipulate the position of the stage.

Experiments were run in potentiostatic and galvanostatic modes. In potentiostatic mode a constant potential (−0.8 V) was applied between the graphite felt and the reference electrode. As a result, oxygen was consumed at the maximum rate (limiting current conditions) limited by the oxygen transport rate to the graphite felt. In galvanostatic mode, a constant current was drawn and the potential drifted freely. In this mode the reaction rate was constant. Care was exercised so that the potential did not exceed −0.9 V, below which protons would be reduced causing additional current in the circuit.

The goal of the first experiment (in potentiostatic mode) was to compare the average oxygen flux calculated from the microelectrode measurements for different flow velocities with the "true" flux calculated from polarization current. Dissolved oxygen profiles were collected at 16 different locations above and within the graphite felt. These locations were 4000 μm apart and arranged in a 4×4 matrix. The oxygen flux was calculated for each profile and the average flux from 16 measurements was determined for each flow velocity. The measurements were repeated for the following flow velocities: 0.139, 0.408, 0.456, 1.11, 1.99, 2.30 and 2.78 $cm\ s^{-1}$. In this experiment the mass transport rate of oxygen to the graphite felt changed as the flow velocity changed thus affecting the oxygen reduction rate.

The goal of the second experiment (in galvanostatic mode) was to eliminate the effects of changing mass transport rate at different flow velocities. The current was 0.268 mA and the potential varied from −0.7 to −0.9 V against the SCE. Under such conditions the oxygen flux to the graphite felt was constant, 0.0769 $mg\ s^{-1}\ m^{-2}$ and did not depend on flow velocity. Profiles of dissolved oxygen were collected at a single, arbitrarily selected, location near the center of the graphite felt. *One* oxygen profile was measured for each of the following flow velocities: 0.139, 0.408, 0.694, 1.11, 1.99 and 2.78 $cm\ s^{-1}$. Since the current drawn by the graphite felt was constant, the flux of oxygen evaluated from the microelectrode measurement was expected to be constant. However, for increased flow velocities, the presence of the microelectrode may have influence the results of microelectrode measurements. Although the numerical values of such measurements are likely to be site specific, the position of the site should not change the nature of these interferences in that the effect of the microelectrode will be more visible at high flow velocities than at low flow velocities.

RESULTS AND DISCUSSION

The Reynolds number was calculated for each flow velocity using the mean hydraulic radius as the characteristic length (Bird *et al.*, 1960) and a kinematic viscosity of $1.00 \times 10^{-6}\ m^2\ s^{-1}$ (Gerhart *et al.*, 1992). The results are presented in Table 1.

Figure 2 shows the oxygen flux calculated from microelectrode measurements at various locations above the graphite felt and for various flow velocities in the reactor. The direction of flow is indicated by the arrows next to the *Y*-axis. The measurements were taken in potentiostatic mode using limiting current conditions. Numbers along the *Y*- and *X*-axes indicate the locations where the oxygen profiles were measured. There were 16 different locations organized in a square (4×4) matrix where (1, 1) is the first and (4, 4) is the last measurement sites. The dissolved oxygen concentration in the bulk liquid was 6 $mg\ l^{-1}$ and decreased to zero inside the graphite felt (results not shown). To determine the fluxes of oxygen from the oxygen profiles, the slopes of the steepest linear part of the profile were measured and the result multiplied by the molecular diffusivity of oxygen in water, according to Fick's law of diffusion. The fluxes were different at each location, which reflected the influence of the reactor geometry and, perhaps, the edge effects resulting from the fact that the graphite felt did not cover the whole reactor. Since there was variability among the fluxes evaluated at different locations, the average flux was calculated using all 16 measurements for each flow velocity and this average flux was used as a representative flux calculated from the microelectrode measurements. The average fluxes and the respective standard deviations for each flow velocity are shown in Table 2.

To see the effect of flow velocity on fluxes measured by microelectrodes, the average oxygen flux calculated from the oxygen profiles and the respective flux calculated from the current reading for the same flow velocity, are plotted in Fig. 3. The standard deviation for the microelectrode measurements is indicated by error bars. The graph shows that for the lowest flow velocity (0.139 $cm\ s^{-1}$) the estimated and the true flux were almost the same. When the flow velocity increased, the flux calculated from the oxygen profiles was an overestimate. The deviation of the flux calculated from the oxygen

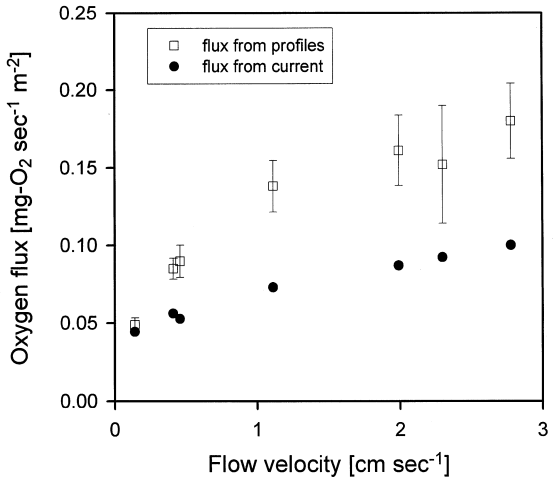


Fig. 3. Average oxygen fluxes calculated from oxygen profiles and from current measurements as function of flow velocity. The standard deviation for the microelectrode measurements is indicated by error bars. Both the standard deviation and the difference between the two fluxes increase with increased flow velocity from zero to 1 cm s^{-1}.

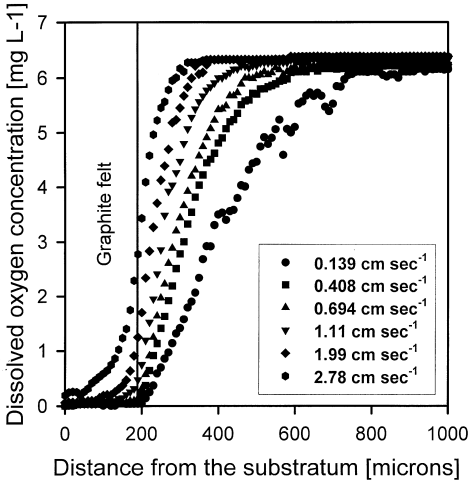


Fig. 5. Oxygen profiles measured at the same location at flow velocities: 0.139, 0.408, 0.694, 1.11, 1.99 and 2.78 cm s^{-1}. The oxygen reduction rate was constant. The slopes increased with increased flow velocity up to 1.11 cm s^{-1}.

profiles (FP) and that calculated from the current (FC), expressed as (FP-FC)/FC, are plotted vs flow velocity in Fig. 4. The difference between the true and the estimated fluxes increases with increased flow velocity up to 1 cm s^{-1} and then remains approximately constant. For flow velocities above 1 cm s^{-1} the difference between the fluxes evaluated from the microelectrode measurements and from the current measurements was consistently 80%. Qualitatively, the latter result compares well with that reported by Glud *et al.* (1994). However, we also demonstrated that for flow velocities below 1 cm s^{-1} the deviation between the "true" flux

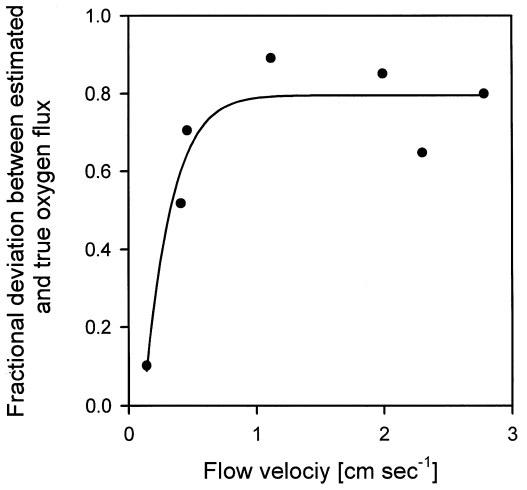


Fig. 4. Oxygen flux calculated from oxygen profiles deviates from the flux calculated using the polarization current. There is a clear dependence between the magnitude of the deviation and the flow velocity between zero and 1.0 cm s^{-1}.

measured from the polarization current and that estimated from the microelectrode measurements was flow velocity dependent; a higher flow velocity resulted in an increased deviation.

The error bars in Fig. 3 show the standard deviation of oxygen flux evaluated from the microelectrode measurements for each flow velocity. When the flow velocity increased from 0.139 to 1.99 cm s^{-1}, the standard deviation increased approximately from 20% to 30% of the average flux. At the flow velocity of 2.30 cm s^{-1} the standard deviation was 50%, but it decreased to about 30% for the velocity of 2.78 cm s^{-1}. We expect that the flux measured for each flow velocity at each location is identical. Therefore, these deviations represent the variability within the sample. Standard deviation increases with increased flow velocity which most likely reflects flow instability at higher flow velocities.

In the second experiment the electrochemical analog of a biofilm was operated in galvanostatic mode. The oxygen flux was set by the constant current drawn from the graphite felt. Consequently, the oxygen flux to the graphite felt should not depend on the flow velocity and should remain constant. To assess if this condition was present in our system, a single oxygen profile was measured at different flow velocities at a single arbitrarily selected point above the graphite felt. The results are shown in Fig. 5. The thickness of the graphite felt we used was 300 microns. However, the point "zero" on the distance scale in Fig. 5 does not mark the position of the bottom. This point was arbitrarily selected within the graphite felt as a common procedure. To prevent electrode tips from breaking, measurements are usually interrupted before the tip reaches the bottom. Moreover, oxygen is often depleted just several microns below the

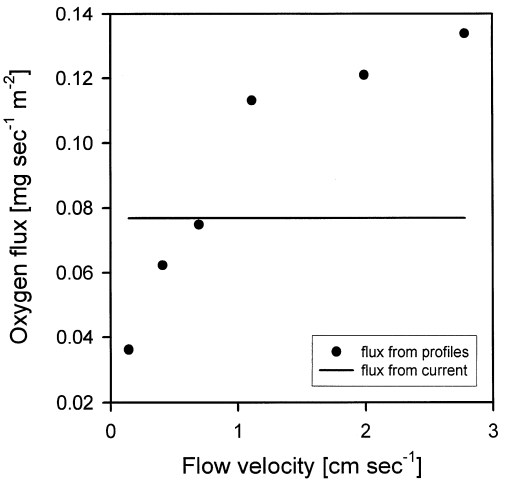


Fig. 6. Oxygen flux calculated from the oxygen profiles in figure 5 and from the constant current applied in the same experiment. The deviation between the two fluxes increases with increased flow velocity up to 1 cm s^{-1}; it remains almost constant beyond this point.

biofilm surface, so there is not much to measure below that point anyway. The surface of the graphite felt was positioned somewhere near 200 microns on the distance scale. Locating the biofilm surface exactly is a difficult task (Lewandowski *et al.*, 1990).

The fluxes calculated from the profiles in Fig. 5 are plotted against the flow velocity in Fig. 6. Each flux (filled circles) in this figure is based on a single oxygen profile and all profiles were measured at the same location. The numerical values, therefore, cannot be compared with the total flux obtained from the current readings (solid line) due to the variability in oxygen reduction rate at different locations on the felt. Measuring oxygen profiles at an arbitrarily selected point is, surely, not the best way to estimate oxygen flux to the entire graphite felt. However, such an approach is sometimes used in microelectrode work with real biofilms where conclusions are drawn about oxygen flux to large surfaces covered with biofilms based on a single measurement at an arbitrarily selected location. The graph shows that even when the flux calculated from the current is forced to be constant, the flux estimated from the microelectrode measurements increases with increasing flow velocity. As in the first experiment we see that the flux calculated from microelectrode measurements is very sensitive to flow velocity below 1 cm s^{-1}.

The distribution of the data shown in Fig. 6 may have hypothetically resulted from some of the simplifying assumptions accepted for calculating oxygen fluxes. It is worth noticing that the oxygen gradients (Fig. 5) measured at the two lowest flow velocities developed entirely outside the graphite felt, while the remaining gradients, measured at higher flow velocities, had their linear portions partially within the graphite felt. To calculate oxygen fluxes we measure gradients of the linear portions of the concentration profiles and multiply these gradients by the molecular diffusivity of oxygen in water. This is a direct application of Fick's first law. In principle, the gradients should be evaluated at the biofilm (graphite felt) surface. Mathematically, concentration profiles above and below the surface are described by different equations; the equations intersect each other at the surface with a common solution satisfying the flux continuity requirement. Since it is well known that evaluating the exact position of a biofilm surface is not trivial (Lewandowski *et al.*, 1990) the entire linear portions of the profiles are usually taken into account and not just the regions adjacent to the interface. Such an approach may result in ignoring possible influences of convective mass transport above the surface and oxygen consumption below the surface on the shape of oxygen profiles. Since the oxygen profiles in Fig. 5, measured at lower flow velocities, developed entirely above the felt surface, their gradients could have been affected by convective mass transport, making them appear less steep. Consequently, calculations of oxygen fluxes may have yielded values lower then expected. The oxygen profiles measured at higher flow velocities, on the other hand, had part of their linear portion within the graphite felt. The gradients evaluated from those profiles could have been affected by oxygen consumption within the felt making them appear steeper. Consequently, calculations of oxygen fluxes may have yielded values higher then expected. It is unclear whether the observed deviations of measured fluxes from expected values was dominated by the above effect, or by interference from the microelectrode present within the boundary layer. It is clear, however, that the commonly accepted procedure for calculating fluxes does not take into consideration possible influence from convection and reaction. Our experiments were designed in such a way that the oxygen flux was essentially constant. If the measured results deviated from expected, it was either because of the interference due to the presence of the microelectrode or because the computational procedures employed to calculate the results were imperfect.

Microelectrode measurements are important for microscale biofilm research and the need to evaluate their reliability is obvious. We found that the fluxes of oxygen evaluated from microelectrode measurements differed from the true fluxes; the fluxes calculated from the microelectrode measurements tended to overestimate the real fluxes. For flow velocities below 1 cm s^{-1} the magnitude of the deviation was sensitive to the flow velocity. For flow velocities between 1 and 3 cm s^{-1} the microelectrode measurements constantly overestimated the oxygen flux by 80%. Our measurements covered only relatively low flow velocities, in the range of zero to 3 cm s^{-1}.

Although these velocities are frequently used in laboratory scale biofilm reactors, future measurements will cover higher flow velocities.

CONCLUSIONS

(1) For flow velocities above 0.4 cm s^{-1} the flux of oxygen to a cathodically polarized graphite felt calculated from oxygen profiles measured by microelectrodes was consistently higher than the true oxygen flux, estimated from the current drawn by the felt.

(2) For flow velocities less than 1 cm s^{-1} the difference between the oxygen flux calculated from oxygen profiles and that calculated from the current depended on flow velocity; the higher the flow velocity the bigger the difference.

(3) For flow velocities between 1 and 3 cm s^{-1} the oxygen fluxes calculated from oxygen profiles consistently overestimated the true oxygen flux by 80%.

(4) Oxygen fluxes calculated from oxygen profiles were both site-dependent and velocity-dependent. When the flow velocity increased, the standard deviation of the oxygen flux calculated from the oxygen profiles measured at different locations also increased.

Acknowledgements—This research was supported by the cooperative agreement (EEC-8907039) between the National Science Foundation and Montana State University-Bozeman. The authors thank Dr Frank Roe, Dr Allan Hamilton and Vicky Allan for valuable comments and suggestions.

REFERENCES

Abrahamson M. T. (1995) Development of artificial biofilms for use in mass transport studies. Master's thesis, MSU Bozeman, MT.

Bird R. B., Stewart W. E. and Lightfoot E. N. (1960) *Transport Phenomena*, p. 188. Wiley, New York.

Brune A., Emerson D. and Breznak J. A. (1995) The termite gut microflora as an oxygen sink: microelectrode determination of oxygen and pH gradients in guts of lower and higher termites. *Appl. Environ. Microbiol.* **61,** 2681–2687.

Chen C. I. and Reinsel M. A. (1996) Characterization of microbial souring in berea-sand porous medium with a north sea oil field inoculum. *Biofouling*. **9,** 175–186.

Chen C. I., Reinsel M. A. and Mueller R. F. (1994) Kinetic investigation of microbial souring in porous media using microbial consortia from oil reservoirs. *Biotechnol. Bioeng*. **44,** 263–269.

Christensen P. B., Nielsen L. P., Revsbech N. P. and Sørensen J. (1989) Microzonation of denitrification activity in stream sediments as studied with a combined oxygen and nitrous oxide microsensor. *Appl. Environ. Microbiol*. **55,** 1234–1241.

Clark L. C., Wolf R., Granger D. and Taylor Z. (1953) Continuous recording of blood oxygen tensions by polarography. *J. Appl. Physiol*. **6,** 189–193.

Cunningham A. B. and Peyton B. M. (1995) In *Applied Bioremediation of Petroleum Hydrocarbons*, ed. R. E. Hinchee, J. A. Kittel and H. J. Reisinger, pp. 97–100. Battelle Press, OH.

Dalsgaard T., de Zwart J., Robertson L. A., Kuenen J. G. and Revsbech N. P. (1995) Nitrification, denitrification and growth in artificial thiosphaera biofilms as measured with combined microsensor for oxygen and nitrous oxide. *FEMS Microbiol. Ecol.* **17,** 137–148.

Dalsgaard T. and Revsbech N. P. (1992) Regulating factors of denitrification in trickling filter biofilms as measured with the oxygen/nitrous oxide microsensor. *FEMS Microbiol. Ecol.* **101,** 151–164.

Dawson D. A. and Trass O. (1972) Mass transfer at rough surfaces. *J. Heat. Mass. Transfer* **15,** 1317–1336.

De Beer D., Stoodley P. and Lewandowski Z. (1996) Liquid flow and mass transport in heterogeneous biofilms. *Water Res*. **30,** 2761–2765.

DeBecker B., Duby P., Modi V. and West A. C. (1995) Mass transfer to a line electrode in presence of a periodic fluid flow. *J. Electrochem. Soc*. **142,** 3001–3007.

Gao X., Lee J. and White H. S. (1995) Natural convection at microelectrodes. *Anal. Chem*. **67,** 1541–1545.

Gerhart P. M., Gross R. J. and Hochstein J. I. (1992) *Fundamentals of Fluid Mechanics*, p. 916. Addison-Wesley, New York.

Glud R. N., Gundersen J. K., Revsbech N. P. and Jørgensen B. B. (1994) Effects on the benthic boundary layer imposed by microelectrodes. *Limnol. Oceanogr*. **39,** 462–467.

Gristina A. G. (1994) Biofilms and chronic bacterial infections. *CMNEEJ* **16,** 171–178.

Hamilton W. A. (1995) In *Microbial Biofilms*, ed. H. M. Lappin-Scott and J. W. Costerton, pp. 171–182. Cambridge University Press, New York.

Hanratty T. J. (1991) Use of the polarographic method to measure wall shear stress. *J. Appl. Electrochem*. **21,** 1038–1046.

Holmes C. J. and Evans R. (1986) Biofilm and foreign body infection — the significance to CAPD-associated peritonitis. *Peritoneal Dial. Bull*. **6,** 168–177.

Højberg O., Revsbech N. P. and Tiedje J. M. (1994) Denitrification in soil aggregates analyzed with microsensors for nitrous oxide and oxygen. *Soil Sci. Soc. Am. J*. **58,** 1691–1698.

Juhasz N. M. and Deen W. M. (1993) Electrochemical measurements of mass transfer at surfaces with discrete reactive areas. *AIChE J*. **39,** 1708–1715.

Larsen T. A. and Harremoës P. (1994) Combined reactor and microelectrode measurements in laboratory grown biofilms. *Water Res*. **28,** 1435–1441.

Lee W., Lewandowski Z., Nielsen P. H. and Hamilton W. A. (1995) Role of sulfate-reducing bacteria in corrosion of mild steel: a review. *Biofouling*. **8,** 165–194.

Lewandowski Z., Altobelli S. A. and Fukushima E. (1993) NMR and microelectrode studies of hydrodynamics and kinetics in biofilms. *Biotechnol. Prog*. **9,** 40–45.

Lewandowski Z., Lee W. C., Characklis W. G. and Little B. (1989) Dissolved oxygen and pH microelectrode measurements at water-immersed metal surfaces. *Corrosion* **45,** 92–98.

Lewandowski Z., Stoodley P. and Roe F. (1995) Internal mass transport in heterogeneous biofilms recent advances. In *Corrosion '95*, Orlando, FL, 1995. NACE, Paper 222.

Lewandowski Z., Stoodley P. and Altobelli S. (1995b) Experimental and conceptual studies on mass transport in biofilms. *Water Sci. Tech*. **31,** 153–162.

Lewandowski Z., Walser G., Larsen R., Peyton B. and Characklis W. G. (1990) Biofilm surface positioning. In *Conference of the American Society of Civil Engineers Arlington, VA, July 8-11, 1990*. Environmental Engineering Division, Environmental Engineering Proceedings, pp. 17–24.

Longmire M. L., Watanabe M., Zhang H., Wooster T. T. and Murray R. W. (1990) Voltammetric measurement

of ultraslow diffusion rates in polymeric media with microdisk electrodes. *Anal. Chem.* **62,** 747–752.

Marsh P. D. (1995) In *Microbial Biofilms*, ed. H. M. Lappin-Scott and J. W. Costerton, pp. 282–300. Cambridge University Press, New York.

Nielsen L. P., Christensen P. B., Revsbech N. P. and Sørensen J. (1990a) Denitrification and oxygen respiration in biofilms studied with a microsensor for nitrous oxide and oxygen. *Microb. Ecol.* **19,** 63–72.

Nielsen L. P., Christensen P. B., Revsbech N. P. and Sørensen J. (1990b) Denitrification and photosynthesis in stream sediment studied with microsensor and whole-core techniques. *Limnol. Oceanogr.* **35,** 1135–1144.

Ramsing N. B., Kühl M. and Jørgensen B. B. (1993) Distribution of sulfate-reducing bacteria, O_2, and H_2S in photosynthetic biofilms determined by oligonucleotide probes and microelectrodes. *Appl. Environ. Microbiol.* **59,** 3840–3849.

Revsbech N. P., Christensen P. B., Nielsen L. P. and Sørensen J. (1989) Denitrification in a trickling filter biofilm studied by a microsensor for oxygen and nitrous oxide. *Water Res.* **23,** 867–871.

Revsbech N. P. (1989) An oxygen microsensor with a guard cathode. *Limnol. Oceanogr.* **34,** 474–478.

Sturman P. J., Stewart P. S., Cunningham A. B., Bouwer E. J. and Wolfram J. H. (1995) Engineering scale-up of in situ bioremediation processes: a review. *J. Contaminant Hydrol.* **19,** 171–203.

Yang S. and Lewandowski Z. (1995) Measurement of local mass transfer coefficient in biofilms. *Biotechnol. Bioeng.* **48,** 737–744.

Zhang T. C., Fu Y. C., Bishop P. L., Kupferle M., FitzGerald S., Jiang H. H. and Harmer C. (1995a) Transport and biodegradation of toxic organics in biofilms. *J. Hazardous Mater.* **41,** 267–285.

Zhang T. C., Fu Y. C. and Bishop P. L. (1995b) Competition for substrate and space in biofilms. *Water Environ. Res.* **67,** 992–1003.